

Cite this: *Chem. Sci.*, 2019, 10, 8202 All publication charges for this article have been paid for by the Royal Society of ChemistryReceived 6th May 2019  
Accepted 21st July 2019DOI: 10.1039/c9sc02185j  
rsc.li/chemical-science

# Solid-state Suzuki–Miyaura cross-coupling reactions: olefin-accelerated C–C coupling using mechanochemistry†

Tamae Seo,<sup>a</sup> Tatsuo Ishiyama,<sup>a</sup> Koji Kubota \*<sup>ab</sup> and Hajime Ito \*<sup>ab</sup>

The Suzuki–Miyaura cross-coupling reaction is one of the most reliable methods for the construction of carbon–carbon bonds in solution. However, examples for the corresponding solid-state cross-coupling reactions remain scarce. Herein, we report the first broadly applicable mechanochemical protocol for a solid-state palladium-catalyzed organoboron cross-coupling reaction using an olefin additive. Compared to previous studies, the newly developed protocol shows a substantially broadened substrate scope. Our mechanistic data suggest that olefin additives might act as dispersants for the palladium-based catalyst to suppress higher aggregation of the nanoparticles, and also as stabilizer for the active monomeric Pd(0) species, thus facilitating these challenging solid-state C–C bond forming cross-coupling reactions.

## Introduction

Solid-state organic reactions have attracted considerable interest in a variety of research areas due to their potentially lower environmental impact and the possibility to access reaction pathways that are unavailable in solution.<sup>1,2</sup> In addition, solid-state reactions are particularly useful for substrates that are poorly soluble in common organic solvents.<sup>2</sup> However, the development of highly efficient solid-state organic transformations whose performance is comparable to conventional solvent-based synthetic routes remains challenging.<sup>2</sup> This is mainly due to poor mixing efficiency of the reactants and/or catalysts in the solid state, where organic molecules are arranged tightly and regularly.<sup>2</sup> Thus, the exploration of new strategies and concepts for solid-state organic reactions is of great interest in synthetic chemistry.<sup>1,2</sup>

The Nobel-prize-winning palladium-catalyzed cross-coupling reactions arguably represent the most powerful, versatile, and well-established class of organic transformations.<sup>3</sup> In particular, the Suzuki–Miyaura cross-coupling of aryl halides with organoboron reagents has found wide applications in both academic and industrial settings.<sup>3c–3f</sup> Conventionally, Suzuki–Miyaura cross-coupling reactions are

carried out in organic solvents.<sup>3c–3f</sup> Compared to such solvent-based protocols, solid-state cross-coupling reactions have remained extremely scarce, even though this approach would present the following advantages: (1) solvent waste would be greatly reduced, especially for large-scale syntheses;<sup>1,2</sup> (2) solid-state coupling reactions should be particularly useful for the preparation of carbon-based materials (*e.g.* large poly-aromatic hydrocarbons) that are typically prepared from substrates that are poorly soluble due to strong intermolecular interactions (*e.g.*,  $\pi$ – $\pi$  interactions);<sup>4</sup> and 3) the set-up for solid-state cross-coupling reactions should be much simpler than that of solution-based reactions. Despite these benefits, only a limited number of solid-state Suzuki–Miyaura cross-coupling reactions under mechanochemical conditions using ball milling has been reported.<sup>5–7</sup> Moreover, the scope of these reactions is significantly restricted, *i.e.*, only electron-deficient aryl halides are applicable, and low conversion rates are common. Thus, we have focused on re-designing palladium-based catalyst systems for the development of a broadly applicable solid-state cross-coupling protocol, which may potentially unlock versatile applications for such solid-state syntheses.

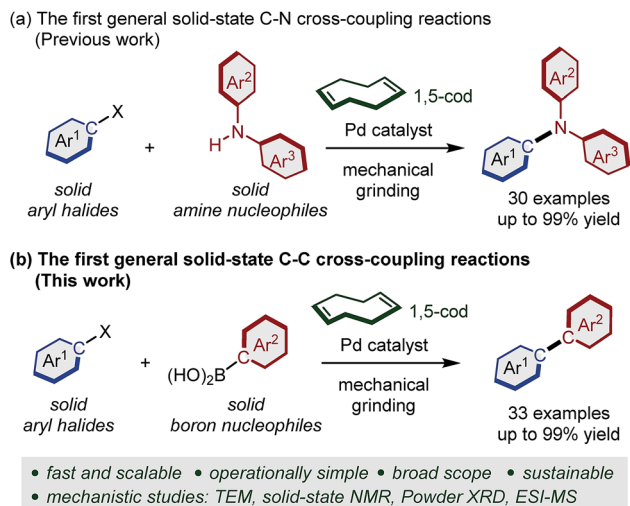
We have previously reported a rational strategy for a general and scalable solid-state Buchwald–Hartwig cross-coupling reaction using mechanochemistry (Scheme 1a).<sup>8</sup> The key finding of this previous study was that olefin additives such as 1,5-cyclooctadiene (1,5-cod) dramatically accelerate the C–N bond-forming reaction in the solid state. Based on a transmission electron microscopy (TEM) analysis, we discovered that olefin additives can act as efficient molecular dispersants for palladium-based catalysts in the solid state, thus inhibiting the deleterious aggregation of the catalyst (Scheme 1a).<sup>8,9</sup>

<sup>a</sup>Division of Applied Chemistry and Frontier Chemistry Center, Faculty of Engineering, Hokkaido University, Sapporo, Hokkaido, Japan. E-mail: hajito@eng.hokudai.ac.jp; kbt@eng.hokudai.ac.jp

<sup>b</sup>Institute for Chemical Reaction Design and Discovery (WPI-ICReDD), Hokkaido University, Sapporo, Hokkaido, Japan

† Electronic supplementary information (ESI) available. See DOI: 10.1039/c9sc02185j



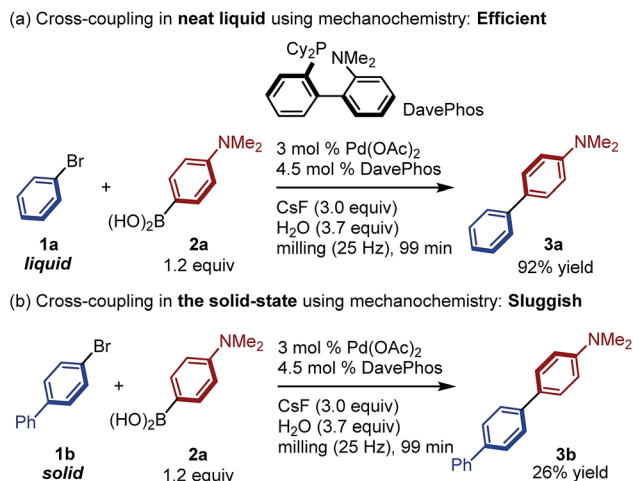


Scheme 1 Olefin-accelerated solid-state cross-coupling reactions using mechanochemistry.

Herein, we report the development of the first general and scalable solid-state Suzuki–Miyaura cross-coupling reactions using mechanochemistry (Scheme 1b). The present study is not a simple extension of our previous work,<sup>8</sup> but represents the development of a new catalytic system for robust C–C bond-forming reaction in the solid-state. Compared to previous studies,<sup>5</sup> the developed system shows a substantially broadened substrate scope and allows the first solid-state organoboron cross-coupling reaction of unactivated aryl chlorides.<sup>5a</sup> Furthermore, we demonstrate the solvent-free solid-state synthesis of large polyaromatic hydrocarbons and a gram-scale mechanochemical synthesis.<sup>4d,10,11</sup> Experimental mechanistic studies to elucidate the roles for the olefin additives in these solid-state cross-coupling reactions are also described.

## Results and discussion

In order to develop a potentially general and scalable solid-state organoboron cross-coupling protocol, we focused on Pd(OAc)<sub>2</sub>/DavePhos, which is a high-performance catalytic system for several cross-coupling reactions developed by Buchwald and co-workers.<sup>11,12</sup> Initially, we compared the reactivity of liquid 1-bromobenzene (**1a**) and solid 4-bromo-1,1'-biphenyl (**1b**) in this mechanochemical palladium-catalyzed Suzuki–Miyaura cross-coupling reaction under slightly modified conditions to those originally used for the solution-based Suzuki–Miyaura coupling reaction (Scheme 2).<sup>12a</sup> Reactions were conducted in a Retsch MM400 mill in a stainless-steel milling jar (1.5 mL) at 25 Hz using one stainless-steel ball (diameter: 5 mm). In the presence of Pd(OAc)<sub>2</sub>/DavePhos, the Suzuki–Miyaura cross-coupling of liquid **1a** with 4-dimethylaminophenylboronic acid (**2a**) proceeded readily to afford the corresponding coupling product (**3a**) in excellent yield (92%; Scheme 2a). In contrast, the reaction of solid **1b** under the same reaction conditions

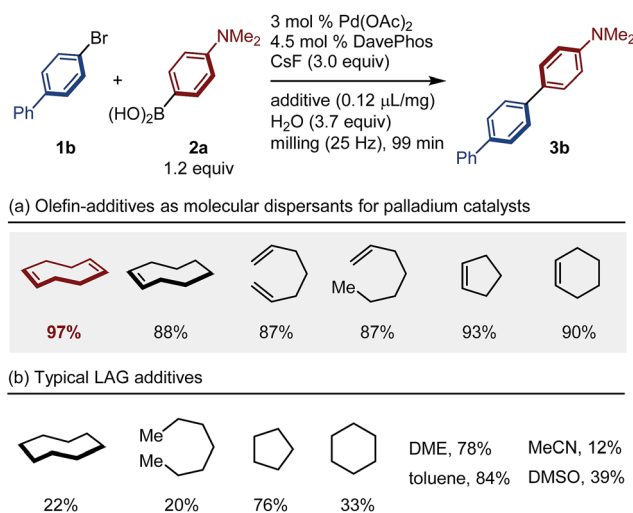


Scheme 2 Reactivity difference between liquid and solid aryl bromides in a Suzuki–Miyaura cross-coupling reaction under solvent-free mechanochemical conditions.

resulted in a low yield of **3b** (26%; Scheme 2b). These results suggest the existence of a considerable reactivity gap between liquid and solid substrates, even under mechanochemical conditions.<sup>8</sup> This is probably due to poor mixing efficiency of the reactants and/or catalysts in the constrained solid-state reaction medium, even under ball-milling conditions.<sup>7</sup>

Given our recent success regarding olefin-accelerated solid-state C–N coupling reactions,<sup>8</sup> we speculated that this strategy could also be potentially applied to solid-state organoboron cross-coupling reactions. Thus, we decided to focus

Table 1 Development of olefin-accelerated solid-state Suzuki–Miyaura cross-coupling using mechanochemistry<sup>a</sup>



<sup>a</sup> Conditions: **1b** (0.3 mmol), **2a** (0.36 mmol), Pd(OAc)<sub>2</sub> (0.009 mmol), DavePhos (0.0135 mmol), CsF (0.9 mmol), H<sub>2</sub>O (20 μL), and additive (0.12 μL mg<sup>-1</sup>) in a stainless-steel ball-milling jar (1.5 mL) with a stainless-steel ball (5 mm).



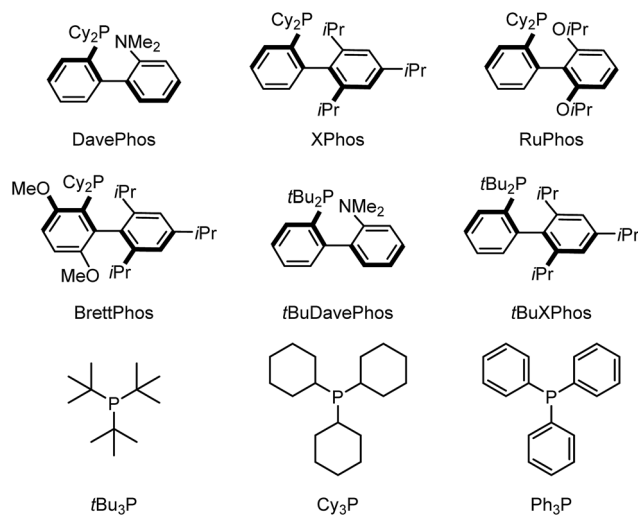
on olefin additives that might act as molecular dispersants for palladium-based catalysts in solid-state media (Table 1). All liquid-assisted grinding (LAG) reactions<sup>13–16</sup> with olefins or other liquid additives were performed at a 0.12 ratio of  $\mu\text{L}$  of liquid added per mg of reactant. The use of olefin additives efficiently promoted the coupling reactions of **1b** with **2a** (Table 1a). In particular, we found that the reaction was dramatically accelerated in the presence of 1,5-cod and the corresponding coupling product **3b** was formed in quantitative yield (97%; Table 1a). In sharp contrast, the use of alkanes or typical organic solvents as LAG additives provided lower yields than those from the reaction with olefins (Table 1b), suggesting that the presence of an olefin functional group is crucial for the observed acceleration. It should be noted that the amount of olefin used in these reactions is comparable to that of the reactant ( $0.12 \mu\text{L mg}^{-1}$ ), which stands in sharp contrast to conventional solution-based coupling reactions, where often a 10- to 100-fold excess of solvent is used.

Subsequently, we investigated the effect of the phosphine ligand on the solid-state organoboron cross-coupling reaction (Table 2). Experiments involving catalyst systems consisting of 3 mol% Pd(OAc)<sub>2</sub> and 4.5 mol% Buchwald-type ligands (Table 2, entries 1–6) revealed that the use of DavePhos provides the desired coupling product in the highest yield (entry 1, 97%). Simple monophosphine ligands such as *t*Bu<sub>3</sub>P, Cy<sub>3</sub>P and Ph<sub>3</sub>P were also examined, but the product yields were moderate (50–70%, entry 7–9). In the absence of a supporting ligand, the reaction provides the product in very low yield (18%, entry 10), suggesting that the use of a phosphine ligand is crucial for this solid-state cross-coupling reaction.

Table 2 Ligand effect on the reaction between **1b** and **2a**<sup>a</sup>

| Entry | Ligand                     | NMR yield (%) |
|-------|----------------------------|---------------|
| 1     | DavePhos                   | 97            |
| 2     | XPhos                      | 65            |
| 3     | RuPhos                     | 92            |
| 4     | BrettPhos                  | 92            |
| 5     | <i>t</i> BuDavePhos        | 82            |
| 6     | <i>t</i> BuXPhos           | 70            |
| 7     | <i>t</i> Bu <sub>3</sub> P | 50            |
| 8     | Cy <sub>3</sub> P          | 60            |
| 9     | Ph <sub>3</sub> P          | 43            |
| 10    | None                       | 18            |

<sup>a</sup> Conditions: **1b** (0.3 mmol), **2a** (0.36 mmol), Pd(OAc)<sub>2</sub> (0.009 mmol), ligand (0.0135 mmol), CsF (0.9 mmol), H<sub>2</sub>O (20  $\mu\text{L}$ ), and 1,5-cod ( $0.12 \mu\text{L mg}^{-1}$ ) in a stainless-steel ball-milling jar (1.5 mL) with a stainless-steel ball (5 mm).



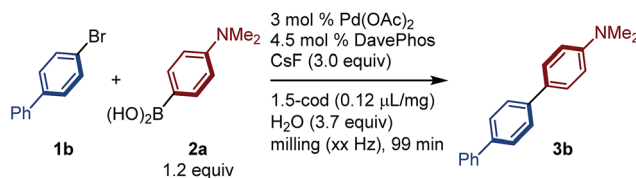
The effect of the mechanochemical reaction parameters on the solid-state organoboron cross-coupling reaction was also investigated (Table 3). For that purpose, the reaction between **1b** and **2a** was performed at different frequency (entries 1–5). The results showed that the product yield increases with increasing frequency, which suggests that the mechanical grinding is important to disperse the substrates, reagents, and catalysts in the solid-state reaction mixture. The use of a smaller ball (entry 6) or a different number of balls (entry 7) did not significantly affect the reactivity of the transformation.

To explore the scope of the present solid-state coupling reaction, a variety of solid aryl halides was tested (Table 4a). This reaction is characterized by a broad substrate scope. The reaction of 2-bromonaphthalene (**1c**) and that of electron-poor aryl bromide **1d** with *p*-methoxyboronic acid (**2b**) proceeded to give the desired products in excellent yield (**3c**: 93%; **3d**: 95%). The developed conditions were also applied to the electron-rich, unactivated solid aryl bromide **1e**, which afforded the desired product (**3e**) in good yield (70%). Aryl bromides containing a thiophene moiety (**1f**) and an internal alkyne (**1g**) also provided the corresponding products in high yield (**3f**: 96%; **3g**: 84%). In addition, aryl bromides containing anthracene (**1h**), fluorene (**1i**), triphenylene (**1j**), tetraphenylethylene (**1k**), and pyrene (**1l** and **1m**) moieties successfully furnished the desired coupling products (**3h–3m**) in moderate to excellent yield (43–94%).

Notably, the developed catalytic system enabled also the solid-state organoboron cross-coupling of unactivated aryl chlorides (Table 4b). The reaction of solid 2-chloronaphthalene (**1c'**) efficiently furnished the desired product (**3c'**; 66%). Aryl chlorides bearing electron-withdrawing groups such as cyano and carbonyl groups also provided the desired products (**3d**, **3n** and **3o**) in high yield (78–95%).

Subsequently, we turned our attention to the scope of solid arylboronic acids (Table 4c). Simple aryl boronic acids afforded the corresponding coupling products (**3p** and **3q**) in good yield (81% and 58%, respectively). Substrates bearing electron-donating groups were coupled efficiently to provide the products (**3r–3u**) in good to excellent yield (87–94%). The product **3r**



Table 3 Investigation on the effect of varying the mechanochemical parameters<sup>a</sup>

| Entry | Frequency (Hz) | Number of balls | Ball size (mm) | NMR yield (%) |
|-------|----------------|-----------------|----------------|---------------|
| 1     | 10             | 1               | 5              | 70            |
| 2     | 15             | 1               | 5              | 75            |
| 3     | 20             | 1               | 5              | 70            |
| 4     | 25             | 1               | 5              | 97            |
| 5     | 30             | 1               | 5              | 99            |
| 6     | 25             | 1               | 3              | 90            |
| 7     | 25             | 2               | 5              | 97            |

<sup>a</sup> Conditions: **1b** (0.3 mmol), **2a** (0.36 mmol), Pd(OAc)<sub>2</sub> (0.009 mmol), DavePhos (0.0135 mmol), CsF (0.9 mmol), H<sub>2</sub>O (20 μL), and 1,5-cod (0.12 μL mg<sup>-1</sup>) in a stainless-steel ball-milling jar (1.5 mL).

was also obtained using the corresponding 4-iodobiphenyl substrate (88%). Substrates bearing electron-withdrawing groups were also compatible with the applied solid-state conditions (**3v–3y**; 57–99%). Finally, this method was successfully applied to the solid-state synthesis of heteroaryl-containing biaryl derivatives (**3z**; 99%).

Under the developed conditions, cross-coupling reactions of diaryl halides in the solid state also proceeded to give the diarylated products in good yield (Table 4d). The reaction of 9,10-dibromoanthracene (**1aa**) with **2b** afforded the double arylation product **3aa** in quantitative yield (99%). Notably, **3aa** could also be successfully synthesized from the corresponding aryl chloride (92%). In addition, this reaction permits the rapid construction of 2,1,3-benzothiadiazole derivatives, which are  $\pi$ -conjugated molecules that are frequently encountered in dye-sensitized solar cells.<sup>17</sup> Specifically, the reaction of dibromo-substituted 2,1,3-benzothiadiazole (**1ab**) furnished a symmetrical D–A– $\pi$ –A–D system in good yield (**3ab**: 60%).

We expected this solid-state organoboron cross-coupling reaction to be particularly useful for the preparation of carbon-based materials that are poorly soluble substrates (e.g. large polyaromatic hydrocarbons) due to strong intermolecular interactions.<sup>4</sup> Therefore, we carried out a preliminary investigation on the construction of polyaromatic hydrocarbons *via* solid-state cross-coupling reactions using mechanochemistry (Table 4e). Structurally complex polyaromatic hydrocarbons (**3ac–3ag**) were successfully synthesized in good to high yield (59–92%). Conventional solvent-based coupling conditions<sup>9</sup> for the preparation of such polyaromatic hydrocarbons often require the use of significant amounts of solvent (<0.05 M), high temperatures, and long reaction times, thus highlighting the synthetic utility of the solid-state cross-coupling method presented herein.

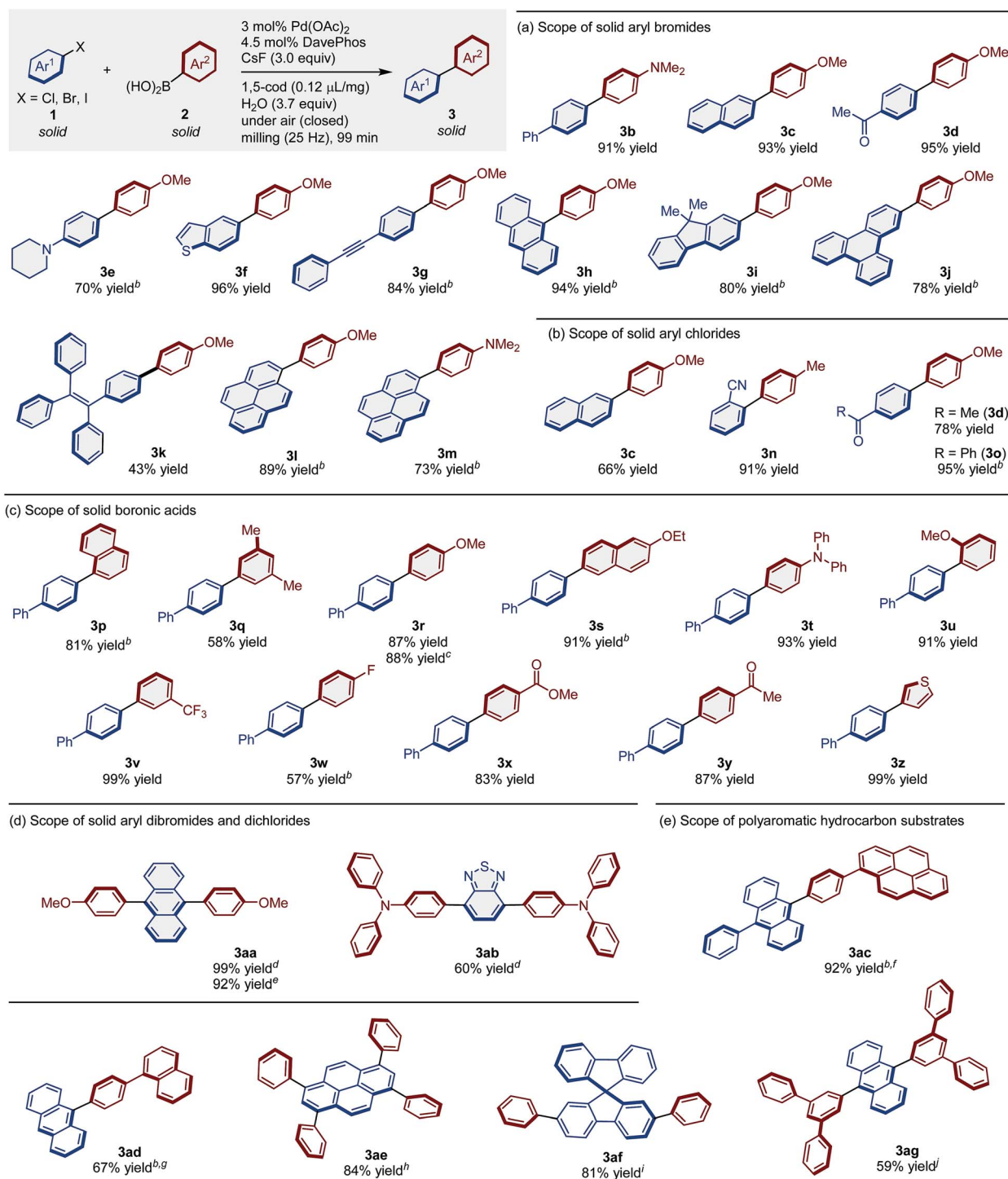
In order to further explore the synthetic utility of this protocol, we conducted a solid-state cross-coupling reaction on the gram-scale under mechanochemical conditions (Fig. 1). The

solid-state cross-coupling of 9-bromoanthracene (**1h**) with **2b** was carried out at an 8.0 mmol scale in a stainless-steel ball-milling jar (25 mL) using four stainless-steel balls (diameter: 10 mm), which afforded **3h** in high yield (87%). The product could be isolated by simple re-precipitation from CH<sub>2</sub>Cl<sub>2</sub>/MeOH. For comparison, we also carried out a solution-based Suzuki–Miyaura cross-coupling reaction in dioxane<sup>12a</sup> at high reaction temperature (100 °C) using a large amount of solvent (160 mL, 0.05 M) and prolonged reaction time (24 h); however, under these conditions, **3h** was obtained only in a moderate yield (52%).<sup>18</sup> It should be noted that solution-based reactions of insoluble aromatic substrates such as **1h** typically require significant amounts of dry solvent, an inert atmosphere, high-vacuum instrumentation, and large reaction flasks equipped with a reflux condenser and an oil bath on a stirring hotplate (Fig. 1).<sup>10</sup> Compared to such complex set-ups, the present solid-state coupling reactions can be carried out in a small jar in air,<sup>19</sup> and special operational skills are not required (for the details of the procedure, see the ESI†). This operational simplicity is likely to substantially increase the practical utility of the present solvent-free solid-state cross-coupling reactions beyond the laboratory scale.

To gain mechanistic insight into the observed acceleration effect upon the addition of olefin additives, we used TEM imaging to characterize the palladium nanoparticles generated *in situ* in the crude reaction mixture of **1b** with **2a** (Fig. 2). The observed image clearly shows the formation of palladium nanoparticles (approximate size: 3–5 nm) in the reaction mixture in the presence of 1,5-cod (Fig. 2B). Notably, higher aggregation of the palladium particles was not observed. On the other hand, the image obtained for the palladium species derived from the reaction mixture in the presence of cyclooctane (Fig. 2C) and in the absence of any additive (Fig. 2D) shows that the palladium species have significantly aggregated into dense particles (Fig. 2C and 2D). These results suggest that olefin additives might act as dispersants for the palladium-



Table 4 Substrate scope of the olefin-accelerated solid-state organoboron cross-coupling



<sup>a</sup> Reaction conditions:  $\text{Pd(OAc)}_2$  (0.009 mmol), DavePhos (0.0135 mmol), **1** (0.3 mmol), **2** (0.36 mmol), CsF (0.9 mmol),  $\text{H}_2\text{O}$  (20  $\mu\text{L}$ ), 1,5-cod (0.12  $\mu\text{L mg}^{-1}$ ) in a stainless-steel ball-milling jar (1.5 mL) with a stainless-steel ball (diameter: 5 mm), 25 Hz, 99 min. Isolated yields are shown. <sup>b</sup> 1,5-Cod (0.2  $\mu\text{L mg}^{-1}$ ) was used. <sup>c</sup> The corresponding aryl iodide was used as the substrate. <sup>d</sup> Reaction conditions:  $\text{Pd(OAc)}_2$  (0.009 mmol), DavePhos (0.0135 mmol), **1** (0.15 mmol), **2** (0.36 mmol), CsF (0.9 mmol),  $\text{H}_2\text{O}$  (20  $\mu\text{L}$ ), 1,5-cod (0.2  $\mu\text{L mg}^{-1}$ ) in a stainless-steel ball-milling jar (1.5 mL) with a stainless-steel ball (diameter: 5 mm), 25 Hz, 99 min. <sup>e</sup> The corresponding aryl chloride was used as the substrate. <sup>f</sup> Reaction time: 180 min. <sup>g</sup> 0.2 mmol scale. <sup>h</sup> Reaction conditions:  $\text{Pd(OAc)}_2$  (0.036 mmol), DavePhos (0.054 mmol), **1** (0.3 mmol), **2** (4.8 mmol), CsF (3.6 mmol),  $\text{H}_2\text{O}$  (80  $\mu\text{L}$ ), 1,5-cod (0.2  $\mu\text{L mg}^{-1}$ ) in a stainless-steel ball-milling jar (25 mL) with stainless-steel balls (diameter: 4  $\times$  10 mm), 25 Hz, 99 min. <sup>i</sup> Reaction conditions:  $\text{Pd(OAc)}_2$  (0.018 mmol), DavePhos (0.027 mmol), **1** (0.3 mmol), **2** (2.4 mmol), CsF (1.8 mmol),  $\text{H}_2\text{O}$  (40  $\mu\text{L}$ ), 1,5-cod (0.2  $\mu\text{L mg}^{-1}$ ) in a stainless-steel ball-milling jar (5 mL) with a stainless-steel ball (diameter: 10 mm), 25 Hz, 180 min. <sup>j</sup> Reaction conditions:  $\text{Pd(OAc)}_2$  (0.03 mmol), DavePhos (0.045 mmol), **1** (0.3 mmol), **2** (0.72 mmol), CsF (1.8 mmol),  $\text{H}_2\text{O}$  (40  $\mu\text{L}$ ), 1,5-cod (0.2  $\mu\text{L mg}^{-1}$ ) in a stainless-steel ball-milling jar (5 mL) with a stainless-steel ball (diameter: 10 mm), 25 Hz, 99 min.



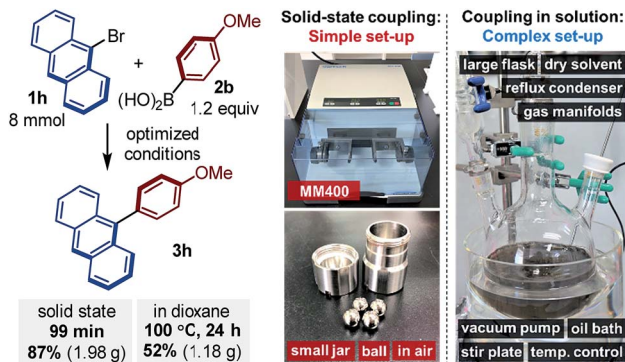


Fig. 1 Solid-state coupling reaction on the gram scale (for detailed reaction conditions, see the ESI†).

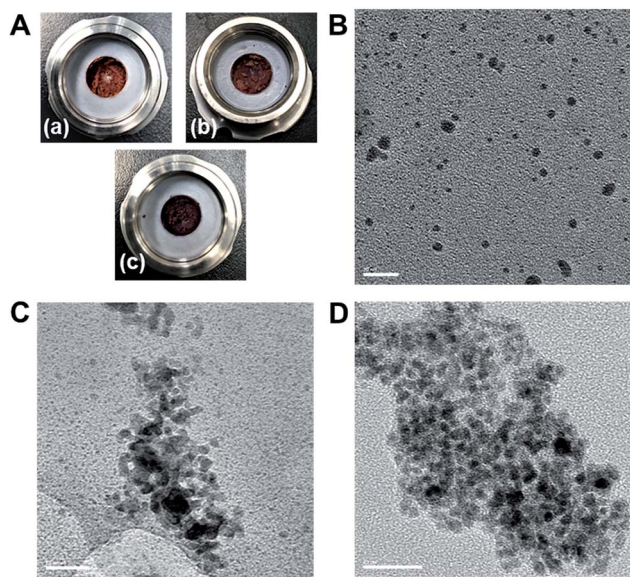


Fig. 2 (A) Reaction mixtures after grinding in a ball mill. Aggregation in the ball mill (a) after 99 min in the presence of 1,5-cod, (b) after 99 min in the presence of cyclooctane, and (c) after 99 min in the absence of an additive. TEM images of the palladium nanoparticles in the crude reaction mixtures: (B) after 99 min in the presence of 1,5-cod, (C) after 99 min in the presence of cyclooctane, and (D) after 99 min in the absence of an additive. Scale bar in the TEM images (bottom left): 20 nm.

based catalyst to suppress higher aggregation of the nanoparticles.<sup>8,9</sup>

Subsequently, we used solid-state (SS)  $^{31}\text{P}$  NMR spectroscopy to examine if monomeric catalytic active species are formed during the cross-coupling reaction in the solid state (Fig. 3). The SS  $^{31}\text{P}$  NMR spectra of the reaction mixtures of 2-bromonaphthalene (**1c**) and *p*-methoxyboronic acid (**2b**) after grinding (25 Hz) in a ball mill in the presence of 1,5-cod showed that signals derived from DavePhos (−14.0 and −16.3 ppm) had completely disappeared, and only one signal (37.6 ppm) was observed, suggesting that a DavePhos-ligated monomeric palladium species is most likely generated (Fig. 3A and B). This is consistent with the results of Table 2, which show that the ligands

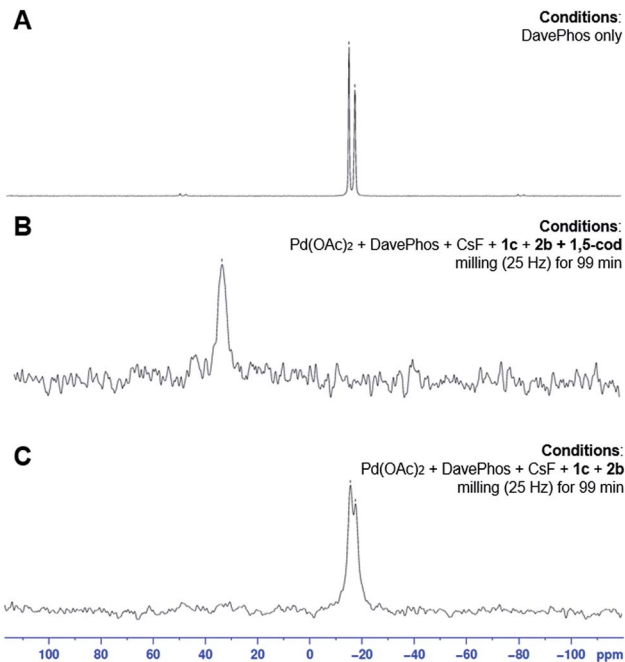
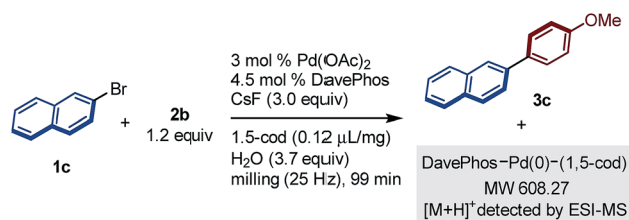


Fig. 3 Analysis of palladium species in the solid-state cross-coupling reaction by solid-state (SS)  $^{31}\text{P}$  NMR. SS  $^{31}\text{P}$  NMR spectra of (A) DavePhos, (B) the reaction mixtures of **1c** and **2b** after grinding in a ball mill in the presence of 1,5-cod, and (C) the reaction mixtures of **1c** and **2b** after grinding in a ball mill in the absence of 1,5-cod.



Scheme 3 ESI mass analysis of the reaction mixture of **1c** and **2b** after grinding in a ball mill in the presence of 1,5-cod. Conditions: **1c** (0.3 mmol), **2b** (0.36 mmol), Pd(OAc)<sub>2</sub> (0.009 mmol), DavePhos (0.0135 mmol), CsF (0.9 mmol), H<sub>2</sub>O (20 μL), and 1,5-cod (0.12 μL mg<sup>−1</sup>) in a stainless-steel ball-milling jar (1.5 mL) with a stainless-steel ball (5 mm).

significantly affect the reactivity. Notably, the SS  $^{31}\text{P}$  NMR spectra of the reaction mixtures of **1c** and **2b** after grinding (25 Hz) in the absence of 1,5-cod showed only signals derived from DavePhos (Fig. 3C). The crude reaction mixture of **1c** and **2b** after grinding in the presence of 1,5-cod was further characterized by ESI mass spectrometry (Scheme 3). The mass spectrum showed a peak corresponding to DavePhos-Pd(0)-(1,5-cod), which is consistent with the results of the SS  $^{31}\text{P}$  NMR analysis. These results suggest that the monomeric DavePhos-Pd(0)-(1,5-cod) species is most likely the resting state of the catalyst during the solid-state cross-coupling reaction in the presence of 1,5-cod.<sup>20</sup> While such a palladium(0) complex should be unstable under ambient conditions,<sup>19</sup> we speculate that the longevity of this palladium(0) complex might be



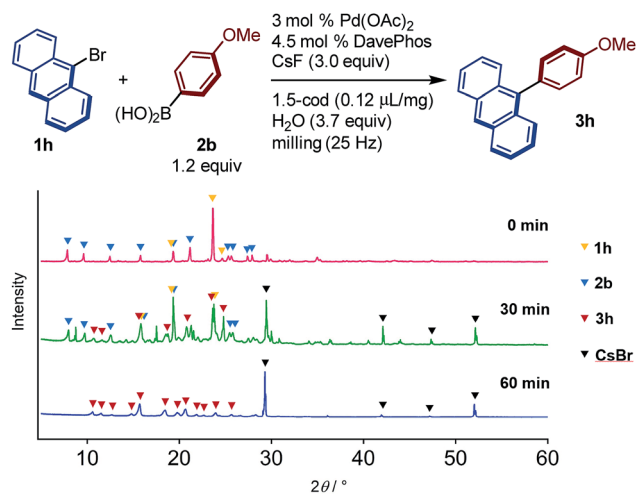


Fig. 4 Monitoring the reaction progress between **1h** and **2b** by PXRD analysis. Conditions: **1h** (0.3 mmol), **2b** (0.36 mmol), Pd(OAc)<sub>2</sub> (0.009 mmol), DavePhos (0.0135 mmol), CsF (0.9 mmol), H<sub>2</sub>O (20 μL), and 1,5-cod (0.12 μL mg<sup>-1</sup>) in a stainless-steel ball-milling jar (1.5 mL) with a stainless-steel ball (5 mm).

rationalized in terms of the low diffusion efficiency of gaseous oxygen in such solid-state reaction mixtures.<sup>21</sup>

The reaction progress of the cross-coupling reaction between **1h** and **2b** in the presence of 1,5-cod was monitored by powder X-ray diffraction (PXRD) analysis (Fig. 4). After 30 min, new diffraction peaks derived from cross-coupling product **3h** and CsBr appeared, while the peaks associated with the starting materials remained. After 60 min, the diffraction peaks derived from the starting materials had been completely disappeared, and only those of coupling product **3b** and CsBr were observed, demonstrating a clean solid-to-solid conversion without melting during the reaction.<sup>8</sup> It should also be noted that a thermographic analysis revealed a temperature of inside the milling jar after

grinding for 99 min at 25 Hz was ~35 °C, which indicates that the temperature did not significantly increase under the applied mechanochemical conditions (see the ESI† for the details).

Based on our mechanistic data, we would like to propose two possible roles for the olefin additives in these solid-state cross-coupling reactions (Fig. 5): (1) olefins might act as dispersants for the palladium-based catalyst to suppress higher aggregation of the nanoparticles, which would lead to catalyst deactivation,<sup>8,9</sup> and (2) the active monomeric Pd(0) species could be stabilized upon coordination by the olefins; subsequently, dissociated Pd(0) species could be coordinated by DavePhos and release the olefin ligands to form [(DavePhos)Pd(0)], which could activate the C–X bond of aryl halides.<sup>8,12,22</sup>

## Conclusions

In summary, we have developed the first general and scalable solid-state Suzuki–Miyaura cross-coupling reaction using mechanochemistry. While few examples of mechanochemical palladium-catalyzed coupling reactions of solid substrates have already been reported, their scope is significantly limited, and they typically exhibit low conversion rates. However, we discovered that the addition of small amounts of olefins dramatically improves the progress of these challenging solid-state C–C bond-forming cross-coupling reactions. Although the use of solvents during work up and/or purification remains a future challenge, the development of our solvent-free solid-state cross-coupling reaction constitutes a significant step in developing industrially attractive and environmentally friendly routes to a broad variety of synthetic targets.

## Conflicts of interest

There are no conflicts to declare.

## Acknowledgements

This work was financially supported by the Japan Society for the Promotion of Science (JSPS) via KAKENHI grants JP18H03907, JP17H06370 and JP19K15547 as well as by the Institute for Chemical Reaction Design and Discovery (ICReDD), which has been established by the World Premier International Research Initiative (WPI), MEXT, Japan. We would like to thank Mr Naoya Nakagawa for his help analysing the solid-state NMR. We would like to thank Ms. Nozomi Takeda for her help analysing the ICP-AES.

## Notes and references

- (a) D. J. C. Constable, C. Jimenez-Gonzalez and R. K. Henderson, *Org. Process Res. Dev.*, 2007, **11**, 133; (b) J. H. Clark and S. J. Tavener, *Org. Process Res. Dev.*, 2007, **11**, 149; (c) J. M. DeSimone, *Science*, 2002, **297**, 799.
- (a) *Solvent-free organic synthesis*, ed. K. Tanaka, Wiley-VCH, Weinheim, 2009; (b) *Organic solid-state reactions*, ed. F. Toda, Springer, 2004; (c) F. Toda, *Acc. Chem. Res.*, 1995, **28**, 480; (d) K. Tanaka and F. Toda, *Chem. Rev.*, 2000, **100**, 480.

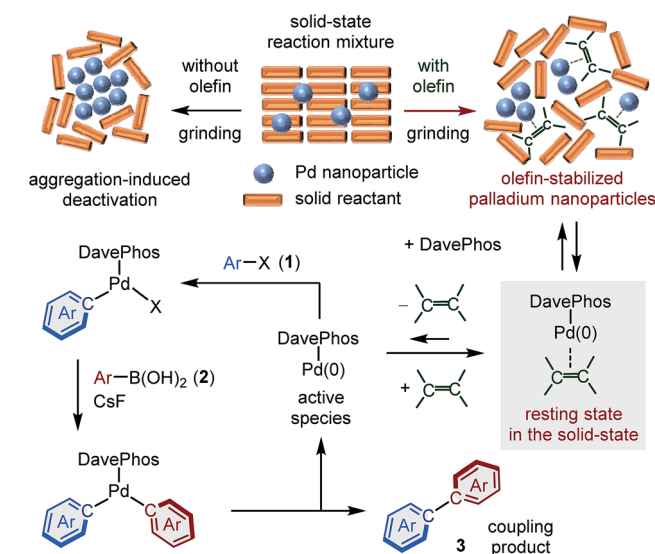


Fig. 5 Proposed reaction mechanism of the solid-state cross-coupling reactions.



- 3 (a) C. C. C. Johansson Seehurn, M. O. Kitching, T. J. Colacot and V. Snieckus, *Angew. Chem., Int. Ed.*, 2012, **51**, 5062; (b) *Palladium-catalyzed coupling reactions: Practical aspects and future developments*, ed. Á. Molnár, Wiley-VCH, Weinheim, 2013; (c) *Metal-catalyzed cross-coupling reactions*, ed. A. Meijere and F. Diederich, Wiley-VCH, Weinheim, 2nd revised edn, 2008; (d) N. Miyaura and A. Suzuki, *Chem. Rev.*, 1995, **95**, 2457; (e) A. J. J. Lennox and G. C. Lloyd-Jones, *Chem. Soc. Rev.*, 2014, **43**, 412; (f) R. Martin and S. L. Buchwald, *Acc. Chem. Res.*, 2008, **41**, 1461.
- 4 (a) L. Chen, Y. Hernandez, X. Feng and K. Müllen, *Angew. Chem., Int. Ed.*, 2012, **51**, 7640; (b) L. T. Scott, E. A. Jackson, Q. Zhang, B. D. Steinberg, M. Bancu and B. Li, *J. Am. Chem. Soc.*, 2012, **134**, 107; (c) G. Povie, Y. Segawa, T. Nishihara, Y. Miyauchi and K. Itami, *Science*, 2017, **356**, 172; (d) K. Kawasumi, Q. Zhang, Y. Segawa, L. T. Scott and K. Itami, *Nat. Chem.*, 2013, **5**, 739; (e) Y. Koga, T. Kaneda, Y. Saito, K. Murakami and K. Itami, *Science*, 2018, **359**, 435.
- 5 For examples of solvent-free solid-state Suzuki–Miyaura cross-coupling reactions using mechanochemistry, see: (a) G. Cravotto, D. Garella, S. Tagliapietra, A. Stolle, S. Schüßler, S. E. S. Leonhardt and B. Ondruschka, *New J. Chem.*, 2012, **36**, 1304; (b) F. Schneider and B. Ondruschka, *ChemSusChem*, 2008, **1**, 622; (c) S. F. Nielsen, D. Peters and O. Axelsson, *Synth. Commun.*, 2000, **30**, 3501; (d) E. N. Leadbeater and M. L. Klingsmith, *Tetrahedron Lett.*, 2003, **44**, 765.
- 6 For examples of solvent-free Suzuki–Miyaura cross-coupling reactions of liquid substrates using mechanochemistry, see: (a) F. Schneider, A. Stolle, B. Ondruschka and H. Hopf, *Org. Process Res. Dev.*, 2009, **13**, 44; (b) Z.-J. Jiang, Z.-H. Li, J.-B. Yu and W.-K. Su, *J. Org. Chem.*, 2016, **81**, 10049.
- 7 For recent reviews on organic syntheses using mechanochemistry, see: (a) S. L. James, C. J. Adams, C. Bolm, D. Braga, P. Collier, T. Friščić, F. Grepioni, K. D. M. Harris, G. Hyett, W. Jones, A. Krebs, J. Mack, L. Maini, A. G. Orpen, I. P. Parkin, W. C. Shearouse, J. W. Steed and D. C. Waddell, *Chem. Soc. Rev.*, 2012, **41**, 413; (b) G.-W. Wang, *Chem. Soc. Rev.*, 2013, **42**, 7668; (c) T. Friščić, I. Halasz, V. Štrukil, M. Eckert-Maksić and R. E. Dinnebier, *ACS Cent. Sci.*, 2017, **3**, 13; (d) J. G. Hernández and C. Bolm, *J. Org. Chem.*, 2017, **82**, 4007; (e) J. G. Hernández, *Chem.–Eur. J.*, 2017, **23**, 17157; (f) T.-X. Métro, J. Martinez and F. Lamaty, *ACS Sustainable Chem. Eng.*, 2017, **5**, 9599; (g) T. K. Achar, A. Bose and P. Mal, *Beilstein J. Org. Chem.*, 2017, **13**, 1907; (h) J.-L. Do and T. Friščić, *Synlett*, 2017, **28**, 2066; (i) D. Tan and T. Friščić, *Eur. J. Org. Chem.*, 2018, **18**; (j) O. Eguagie, J. S. Vyle, P. F. Conlon, M. A. Gilea and Y. Liang, *Beilstein J. Org. Chem.*, 2018, **14**, 955; (k) J. L. Howard, Q. Cao and D. L. Browne, *Chem. Sci.*, 2018, **9**, 3080; (l) J. Andersen and J. Mack, *Green Chem.*, 2018, **20**, 1435; (m) N. R. Rightmire and T. P. Hanusa, *Dalton Trans.*, 2016, **45**, 2352; (n) M. Leonardi, M. Villacampa and J. C. Menéndez, *Chem. Sci.*, 2018, **9**, 2042; (o) C. Xu, S. De, A. M. Balu, M. Ojeda and R. Luque, *Chem. Commun.*, 2015, **51**, 6698; (p) D. Tan and T. Friščić, *Chem. Commun.*, 2016, **52**, 7760; (q) A. A. Gečiąuskaitė and F. García, *Beilstein J. Org. Chem.*, 2017, **13**, 2068; (r) M. J. Muñoz-Bastista, D. Rodríguez-Padron, A. R. Puente-Santiago and R. Luque, *ACS Sustainable Chem. Eng.*, 2018, **9**, 9530; (s) J. Andersen and J. Mack, *Green Chem.*, 2018, **20**, 1435; (t) E. Colacino, M. Carta, G. Pia, A. Porcheddu, P. C. Ricci and F. Delogu, *ACS Omega*, 2018, **3**, 9196; (u) D. Tan and T. Friščić, *Eur. J. Org. Chem.*, 2018, **1**, 18; (v) D. Tan and F. García, *Chem. Soc. Rev.*, 2019, **48**, 2274; (w) C. Bolm and J. D. Hernández, *Angew. Chem., Int. Ed.*, 2019, **58**, 3285.
- 8 K. Kubota, T. Seo, K. Koide, Y. Hasegawa and H. Ito, *Nat. Commun.*, 2019, **10**, 111.
- 9 I. J. S. Fairlamb, *Org. Biomol. Chem.*, 2008, **6**, 3645.
- 10 For selected examples of Suzuki–Miyaura cross-coupling reactions for the synthesis of polyaromatic hydrocarbons under solvent-based conditions, see: (a) J. Huang, B. Xu, J.-H. Su, H. C. Chen and H. Tian, *Tetrahedron*, 2010, **66**, 7577; (b) B. Kobin, S. Behren, B. Braun-Cula and S. Hecht, *J. Phys. Chem. A*, 2016, **120**, 5474; (c) S.-K. Kim, B. Yang, Y. Ma, J.-H. Lee and J.-W. Park, *J. Mater. Chem.*, 2008, **18**, 3376; (d) S. Jeelani Basha, R. Venkatachalam, V. Babu and S. Sethuraman, *Beilstein J. Org. Chem.*, 2013, **9**, 698; (e) H. Lee, B. Kim, S. Kim, J. Kim, J. Lee, H. Shin, J.-H. Lee and J. Park, *J. Mater. Chem. C*, 2014, **2**, 4737.
- 11 J.-P. Corbet and G. Mignani, *Chem. Rev.*, 2006, **106**, 2651.
- 12 (a) D. W. Old, J. P. Wolfe and S. L. Buchwald, *J. Am. Chem. Soc.*, 1998, **120**, 9722; (b) R. Martin and S. L. Buchwald, *Acc. Chem. Res.*, 2008, **41**, 1461; (c) A. C. Sather and S. L. Buchwald, *Acc. Chem. Res.*, 2016, **49**, 2146.
- 13 The selected example of liquid-assisted grinding, see: T. Friščić, S. L. Childs, S. A. A. Rizvi and W. Jones, *CrystEngComm*, 2009, **11**, 418.
- 14 The selected example of ion- and liquid-assisted grinding, see: T. Friščić, D. G. Reid, I. Halasz, R. S. Stein, R. E. Dinnebier and M. J. Duer, *Angew. Chem., Int. Ed.*, 2010, **49**, 712.
- 15 The selected example of vapour-assisted-grinding, see: C. Jia, J. Wang, X. Feng, Q. Lin and W. Tuan, *CrystEngComm*, 2014, **16**, 6552.
- 16 The selected examples of polymer-assisted-grinding, see: (a) D. Hasa, G. S. Rauber, D. Voinovich and W. Jones, *Angew. Chem., Int. Ed.*, 2015, **54**, 7371; (b) D. Hasa, E. Carlino and W. Jones, *Cryst. Growth Des.*, 2016, **16**, 1772.
- 17 (a) J. Hou, H.-Y. Chen, S. Zhang, G. Li and Y. Yang, *J. Am. Chem. Soc.*, 2008, **130**, 16144; (b) Z. Yao, M. Zhang, H. Wu, L. Yang, R. Ki and P. Wang, *J. Am. Chem. Soc.*, 2015, **130**, 16144; (c) J. Zhang, W. Chen, A. J. Rojas, E. V. Jucov, T. V. Timofeeva, T. C. Parker, S. Barlow and S. R. Marder, *J. Am. Chem. Soc.*, 2013, **135**, 16376.
- 18 When the solution-based reaction was carried out at room temperature, the product yield was significantly lower (33% NMR yield).
- 19 The reaction under an atmosphere of Ar provided a similar result as the reaction conducted in air, suggesting that the presence/absence of oxygen is not crucial for the reaction, which is another advantage of this method.



- 20 For structure and reactivity of  $[(\text{LPd})n(1,5\text{-cod})]$  complexes, see: H. G. Lee, P. J. Milner, M. T. Colvin, L. Andreas and S. L. Buchwald, *Inorg. Chim. Acta*, 2014, **422**, 188.
- 21 We have also attempted to prepare the DavePhos-Pd(0)-(1,5-cod) complex via the reaction of  $(1,5\text{-cod})\text{Pd}(\text{CH}_2\text{TMS})_2$  and DavePhos in pentane, but the complex was probably unstable in solution and decomposed during the reaction. However, the *in situ*  $^{31}\text{P}$  NMR analysis of the reaction in  $d_8$ -toluene showed a signal around 35 ppm, which suggests the formation of the DavePhos-Pd(0)-(1,5-cod) complex. The chemical shift is consistent with the SS  $^{31}\text{P}$  NMR shown in Fig. 3B, suggesting that the observed signal (37.6 ppm) in the SS  $^{31}\text{P}$  NMR would be derived from the DavePhos-Pd(0)-(1,5-cod) complex.
- 22 (a) J. Hu and Y. Liu, *Langmuir*, 2005, **21**, 2121; (b) T. Yurino, Y. Ueda, Y. Shimizu, S. Tanaka, H. Nishiyama, H. Tsurugi, K. Sato and K. Mashima, *Angew. Chem., Int. Ed.*, 2015, **54**, 14437.

